J Mater Sci (2008) 43:7385–7390
DOI 10.1007/s10853-008-2972-8

Dynamic deformation behavior of ultrafine grained aluminum produced by ARB and subsequent annealing

Naoki Takata · Yoshitaka Okitsu · Nobuhiro Tsuji

Received: 5 March 2008 / Accepted: 26 August 2008 / Published online: 18 September 2008

Abstract Commercial purity aluminum (1100-Al) sheets with various grain sizes, ranging from 0.2 to 10 μm, were fabricated through accumulative roll bonding (ARB) and subsequent annealing at various temperatures. Mechanical properties of these materials were examined at various strain rates ranging from 10^{-2} to 10^{3} s^{-1} (from quasi-static deformation to dynamic deformation). Yield strength of the UFG specimens did not change so much when the strain rate changed. Yielding behavior of the UFG Al with grain size of 1.4 μm was characterized by yield-drop phenomenon, which appeared at higher strain rate. It was found that strain-hardening of the Al matrix was significantly enhanced at high strain rates, which was independent of the grain size. Uniform elongation increased with increasing strain rate in the specimens with the grain size larger than 1 μm, while post-uniform elongation increased with increasing strain rate in the submicrometer grain-sized specimens. Consequently, total elongation of all specimens was improved as the strain rate increased.

N. Takata (✉)
Department of Metallurgy and Ceramics Science,
Tokyo Institute of Technology, 2-12-1-S8-8, Oookayama,
Megro-ku, Tokyo 152-8552, Japan
e-mail: ntakata@mtl.titech.ac.jp

Y. Okitsu
Automobile R&D Center, Honda R&D, Co., Ltd.,
4630 Shimotakanezawa, Haga-gun, Haga-machi,
Tochigi 321-3393, Japan

N. Tsuji
Department of Adaptive Machine Systems, Osaka University,
2-1 Yamadaoka, Suita, Osaka 565-0871, Japan

Introduction

Energetic research works have clarified that severe plastic deformation (SPD) of metallic materials is a promising way to produce ultrafine grained (UFG) microstructures with mean grain size smaller than 1 μm [1, 2]. The bulky UFG materials are attractive for engineering application because of their extremely high strength about 3–4 times higher than that of the same materials with conventionally coarse grain sizes of 10–100 μm [1–5]. Recent articles have reported that the UFG or nanostructured materials exhibit peculiar mechanical properties [6–9], which are distinguished from those of ordinary metallic materials. For instance, the UFG or nanostructured materials show larger strain rate sensitivity of flow stress compared with the ordinary metallic materials [8, 10–13]. However, there are still few systematic data concerning the strain rate dependence of mechanical properties of the UFG materials with various grain sizes. In particular, mechanical properties at very high strain rate (corresponding to dynamic deformation) are important for the practical application of the UFG materials, for example, as the automotive bodies to keep the safety in collision.

The purpose of the present study is to clarify the strength and ductility at a wide range of strain rate from 10^{-2} to 10^{3} s^{-1} (from quasi-static deformation to dynamic deformation) of the UFG aluminum with various grain sizes fabricated by the ARB process and subsequent annealing.

Experimental

Commercial purity aluminum (Al–0.51mass%Fe–0.12mass%Si–0.11mass%Cu–0.04mass%Ti–0.01mass%Mn–0.01mass%Mg–0.01mass%Zn: JIS-1100) was provided for the ARB

process in this study. The principle of the ARB process has been reported earlier [2]. The ARB process was conducted up to six cycles (equivalent strain: 4.8) at room temperature without lubrication. The 1100-Al sheets with 1 mm thickness intensely deformed by the ARB process were annealed for 1.8 ks at various temperatures ranging from 150 to 400 °C, in order to change the grain size [5]. Microstructural observation by transmission electron microscopy (TEM) was conducted for the ARB processed and subsequently annealed specimens. Thin foils parallel to the transverse direction (TD) of the sheets were prepared by twin-jet electropolishing in a 150 mL HNO_3 + 300 mL CH_3OH solution. Hitachi H-800 TEM was operated at 200 kV. Tensile test at room temperature was carried out for the sheets with various mean grain sizes at an initial strain rate ranging from 10^{-2} to 10^{3} s^{-1} by using a TS-2000 load sensing block type material test system [14] manufactured by Saginomiya Seisakusyo Inc. In most cases, the tensile test was carried out two or three times for each condition. The specimen used for tensile test was 6 mm in gage length and 2 mm in gage width. Total elongation of the specimens was determined from the displacement during the tensile test measured using the magnetic reluctance method. Actual strain rates were calculated using the time–displacement profiles measured in the tensile test.

Results and discussion

Microstructure

Figure 1 shows TEM microstructures of the 1100-Al specimens ARB processed and subsequently annealed at various temperatures [15]. The symbol d_t in Fig. 1 indicates the mean spacing of boundaries along ND. Hereinafter, d_t is referred as the grain size of the specimen. The 1100-Al sheet severely deformed by the ARB exhibited the lamellar UFG microstructure whose mean spacing was 0.20 μm, which agreed with the microstructure reported previously [2]. The microstructural characterization by electron backscattering diffraction (EBSD) in a scanning electron microscope (SEM) determined that the elongated ultrafine grains were mostly surrounded by high angle boundaries with misorientations larger than 15°. The dislocation substructures were also found in the lamellar UFG microstructure. It was found that the elongated UFG microstructure gradually coarsened and changed into equiaxed microstructure during the post-ARB annealing. The annealing at various temperatures can produce the 1100-Al sheets with various grain sizes ranging from 0.2 to 10 μm. The recovery simultaneously occurs at grain interior during the annealing, so that the dislocation substructures were scarcely recognized in the microstructures annealed at temperature higher than 250 °C. In particular, the equiaxed UFG microstructure with the mean grain size of 1.4 μm was observed in the 1100-Al ARB processed and subsequently annealed at 250 °C, as shown in Fig. 1c. It can be summarized that the UFG microstructures with grain size smaller than 1 μm include dislocation substructures, while there are very few dislocations within the microstructures with mean grain size over 1.4 μm, which is quite similar to recrystallized microstructure.

Yielding behavior

Figure 2 shows nominal stress–strain curves of the specimens at various strain rates ranging from 10^{3} to 10^{-2} s^{-1}. Elastic deformation was removed from the raw data and nominal stress and plastic strain were plotted in Fig. 2. The mean grain size (d_t) was also indicated in the figure. The strength at the same strain rate increased with decreasing the grain size of the 1100-Al specimen. The maximum flow stress increased with increasing strain rate in all grain sizes. The as-ARB processed specimen with the smallest grain size (0.2 μm) performed very high strength of 373 MP at a strain rate of 10^{3} s^{-1}. The flow curves of the 0.2 and 0.63 μm specimens reached to the maximum stress at early

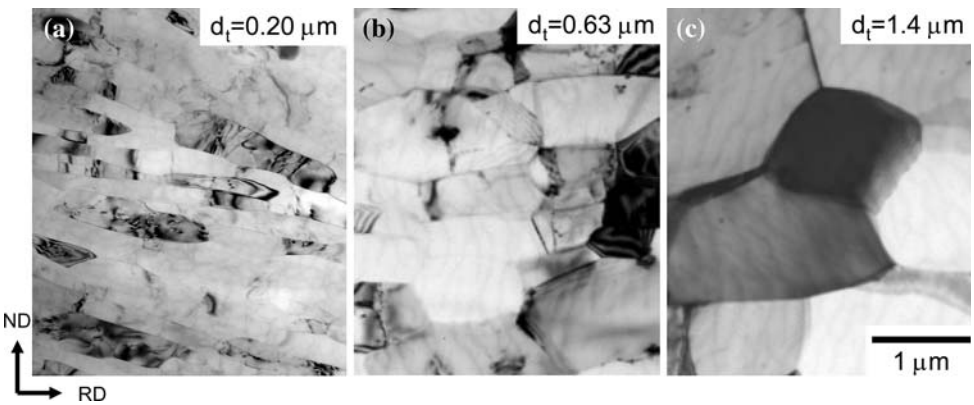

Fig. 1 TEM microstructures of the 1100-Al with various grain sizes produced by the ARB and subsequent annealing at various temperatures. (**a**) As-ARB processed. (**b**) ARB processed and annealed at 200 °C for 1.8 ks. (**c**) ARB processed and annealed at 250 °C for 1.8 ks

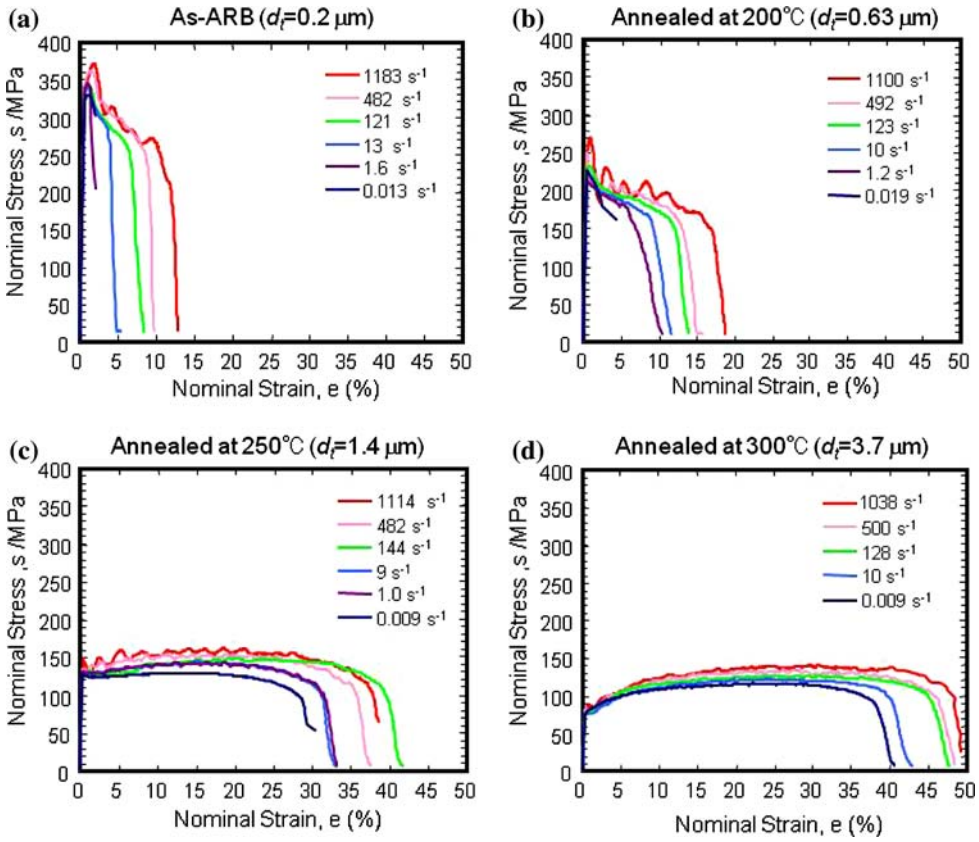

Fig. 2 Nominal stress–strain curves of the 1100-Al with various grain sizes. (**a**) As-ARB processed. $d_t = 0.2$ μm. (**b**) ARB processed and annealed at 200 °C for 1.8 ks. $d_t = 0.63$ μm. (**c**) ARB processed and annealed at 250 °C for 1.8 ks. $d_t = 1.4$ μm. (**d**) ARB processed and annealed at 300 °C for 1.8 ks. $d_t = 3.7$ μm

stage of tensile deformation followed by macroscopic necking, which resulted in limited uniform elongation. In contrast, the specimens having the grain sizes larger than 1 μm showed rather typical stress–strain curves with yielding, strain-hardening, fairly large uniform deformation and necking to failure.

The flow curves at very high strain rates of 5×10^2 and 1×10^3 s^{-1} show oscillations in all specimens, as shown in Fig. 2. It is likely to be caused by the effect of the impact wave generated during the high-speed tensile test. Thus, it should be noted that the oscillated flow curves at high strain rates may not reflect the nature of plastic behaviors of the materials. In order to look at the yielding behaviors carefully, Fig. 3 shows the nominal stress–strain curves in small strain region for the specimens with the mean grain sizes of 1.4 μm (a) and 3.7 μm (b). In the 3.7 μm specimen, the flow curves stress does not change so much even if the strain rate changed greatly. However, the flow curve at a strain rate of 5×10^2 s^{-1} shows an oscillation. Figure 3a shows that a significant oscillation could be recognized at high strain rate of 5.1×10^2 s^{-1} in the 1.4 μm specimen as well. However, the flow curves at relatively low strain rates of 9 and 1.44×10^2 s^{-1} also showed stress drops only at early stage of tensile deformation. Although the change in stress at 482 s^{-1} is again considered to be a stress oscillation due to impact wave, the stress drops below 144 s^{-1} seem to be attributed to a different reason. The previous article [5] has reported that the 1100-Al with the grain sizes about $1 \sim 2$ μm shows the unexpected yield-drop phenomenon at a strain rate 8.3×10^{-4} s^{-1}, which has not yet been reported in pure Al with coarse grain sizes. It can be, therefore, considered that the stress drops of the 1.4 μm specimens at strain rates below 1.44×10^2 s^{-1} recognized in the present study are the yield-drop phenomenon similar to that reported in Ref. [5]. Table 1 shows the initial peak stresses and the following minimum stress at an early stage of tensile deformation at various strain rates for the 1.4 μm specimen. Although the peak stress (upper yield stress) increases with increasing the strain rate, the minimum stress (lower yield stress) is nearly constant independent of the strain rate. This suggests that the yield drop phenomenon can appear more significantly at higher strain rate in the UFG Al. The tendency is in good agreement with the previously reported tendency of well-known discontinuous yielding in mild steels with coarse grain sizes [16].

In order to evaluate the yield strength, the 0.2% proof stresses of the specimens with various grain sizes (d_t) were plotted as a function of strain rate in Fig. 4. A strain rate dependence of the 0.2% proof stress differs depending on the grain size. In the grain size lager than 3.7 μm, the 0.2% proof stress is nearly constant independent of the strain

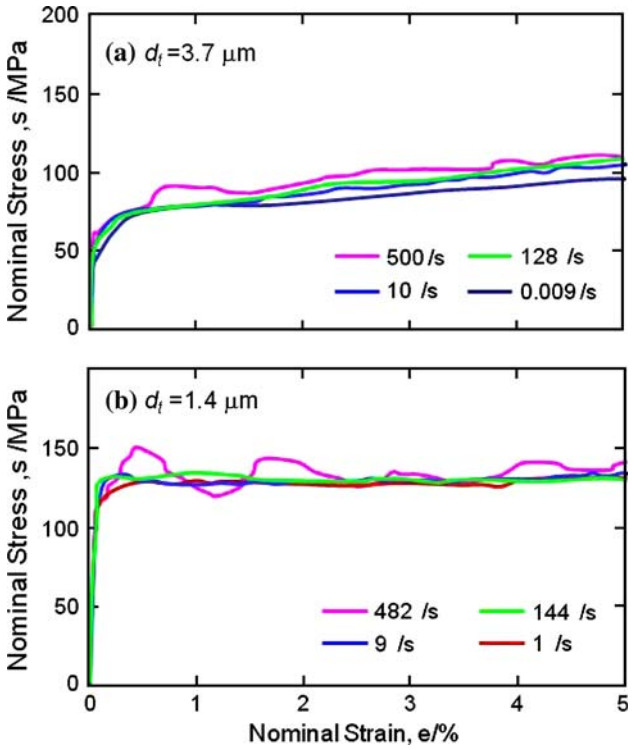

Fig. 3 Nominal stress–strain curves at small strain region for the 1100-Al specimens with the grain sizes of 3.7 μm (**a**) and 1.4 μm (**b**)

Table 1 Initial peak stress and the following minimum stress at an early stage of tensile deformation at various strain rates for the 1100-Al with grain size of 1.4 μm

	Initial strain rate (s^{-1})	0.01	1	10	100	500
d_t = 1.4 μm	0.2% Proof stress (MPa)	127 (0.6)	126 (–)	131 (0.9)	129 (1.4)	144 (11.8)
	Initial peak stress (MPa)	128 (1.4)	129 (–)	131 (0)	133 (0)	152 (1.4)
	Dropped stress (MPa)	126 (0)	127 (–)	128 (2.1)	128 (1.5)	125 (0)

The standard deviations for obtained stresses are indicated in parenthesis

rate. This agrees with the previous knowledge that FCC metals do not show strong strain rate dependency of flow stress [17]. In contrast, the UFG specimens with the mean grain size smaller than 1.4 μm exhibited higher 0.2% proof stress at higher strain rates around 10^3 s^{-1}. However, these are because of the presence of 0.2% stresses on the way to the first peak stress, due to either impact wave oscillation or yield-drop phenomenon, in these specimens. Therefore, it can be concluded that the yield stress of the Al specimens having grain sizes of about 1 μm is independent of the strain rate.

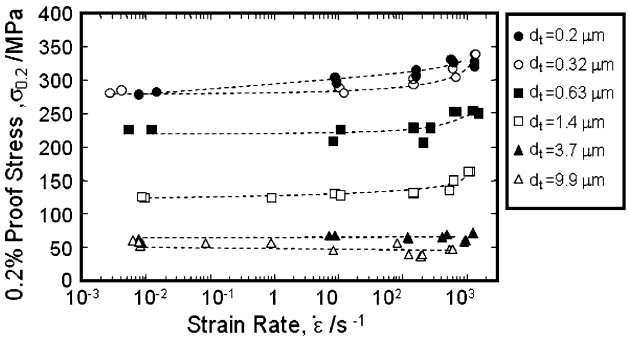

Fig. 4 Change in 0.2% proof stress as a function of strain rate for the 1100-Al specimens with various grain sizes

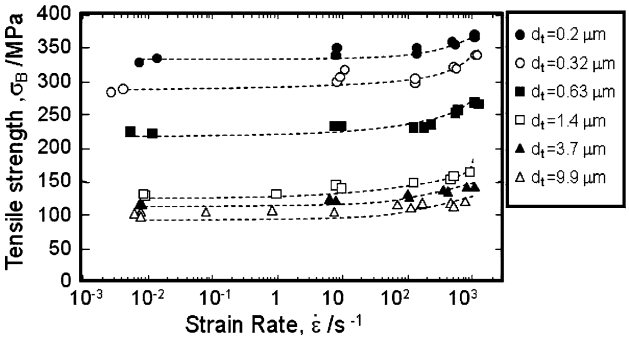

Fig. 5 Tensile strength as a function of strain rate for the 1100-Al specimens with various grain sizes

Plastic deformation behavior after yielding

Figure 5 shows the tensile strength of the specimens with various grain sizes (d_t) as a function of strain rate. The tensile strength slightly increases with increasing strain rate in the range from 10^{-2} to 10 s^{-1}. The increase in tensile strength becomes significant at strain rates above 10^2 s^{-1}. This indicates that the increase in strain rate enhances the strain-hardening of the Al-matrix. It is noteworthy that the difference in the tensile strength between 10^{-2} and 10^3 s^{-1} is nearly constant (about 30 MPa), independent of the grain size.

In order to examine the effect of strain rate on the deformation microstructures, the gauge portion of the specimens tensile deformed at different strain rates was observed in TEM. Figure 6 shows TEM images showing the dislocation substructure in the matrix of the 1100-Al having different grain sizes of 0.2 μm (as-ARB) and 9.9 μm (ARB + annealed at 400 °C) tensile deformed at different strain rates of 10^{-2} and 10^3 s^{-1}. The dislocation substructure composed of ordinary cell boundaries (cell block [18]) was observed in the coarse grained specimen deformed at a low strain rate of 10^{-2} s^{-1}, as shown in Fig. 6a. Dislocation density within the cell blocks was fairly low. The cell structures are thought to be formed

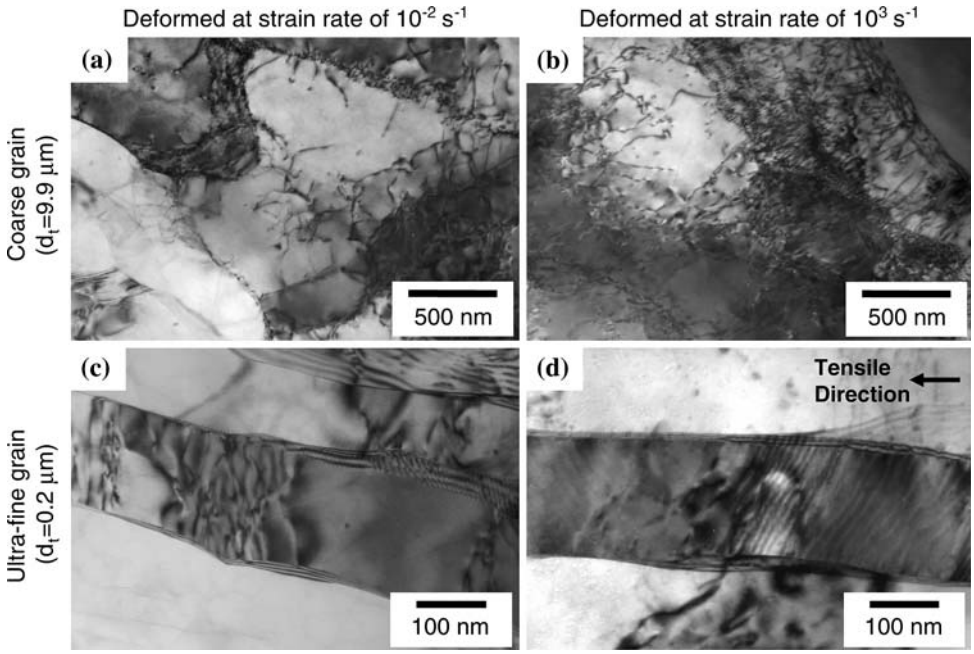

Fig. 6 TEM microstructures showing the dislocation substructures in the 1100-Al specimens with the grain sizes of 9.9 and 0.2 μm after tensile deformation at different strain rates of 10^{-2} and 10^{3} s^{-1}

through dynamic recovery during the tensile test to rearrange the accumulated dislocations [19]. On the contrary, cell substructures were replaced by high-density of tangled dislocations in the specimen deformed at a high strain rate of 10^{3} s^{-1}, as shown in Fig. 6b. The dislocations randomly distributed at the interior of the grains. This verifies that the increase in strain rate can inhibit the annihilation and rearrangement of dislocations, in other words, dynamic recovery. The increase in the tensile strength at high strain rates (Fig. 5) can be explained by the increase in the dislocation density at the interior of the grains. In the UFG 1100-Al ($d_t = 0.2$ μm) deformed at a low strain rate of 10^{-2} s^{-1}, dislocation tangles were seen within the lamella, as shown in Fig. 6c. Since this was the as-ARB processed specimen, there had been some dislocations within the ultra-fine grains even before the tensile test. Compared with the microstructure before the tensile test (Fig. 1a), there is no significant change in the substructures within the elongated UFGs. A remarkable change could be recognized in the UFG specimen deformed at a high strain rate of 10^{3} s^{-1}. That is, significant increase in dislocations within the lamella was found in Fig. 6d. Many parallel dislocations aligned at very small interval within the elongated UFGs. It is evident from the TEM results that the increase in flow stress with increasing strain rate is caused by the strain hardening in both coarse-grained and fine-grained Al. In this sense, it can be concluded that the plastic deformation behavior of the UFG aluminum has a similarity to that of the aluminum with conventional grain size of about 10 μm.

Figure 7 shows the change in total elongation and uniform elongation of the specimens with various grain sizes

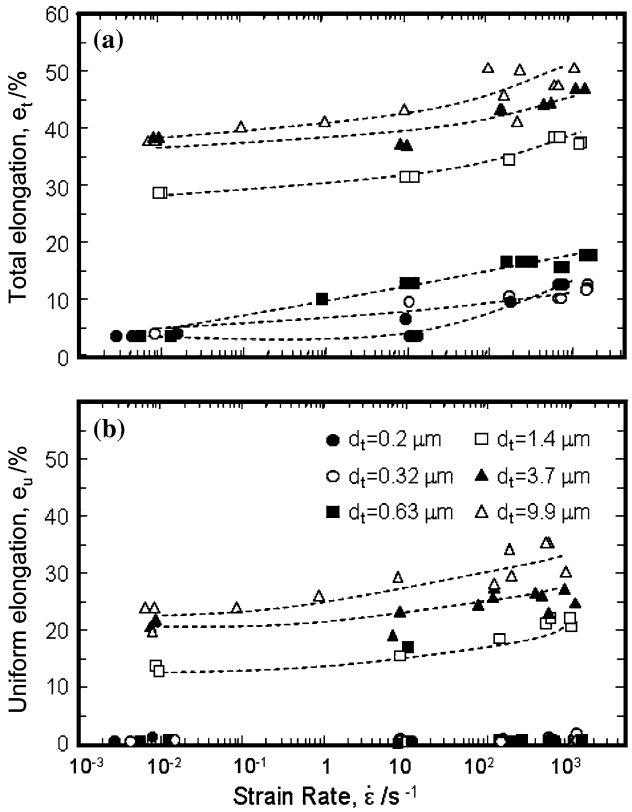

Fig. 7 Total elongation (**a**) and uniform elongation (**b**) as a function of strain rate for the 1100-Al specimens with various grain sizes

as a function of strain rate. The total elongation decreased with decreasing the grain size, especially the decrease was the most significant in the grain sizes ranging from 0.63 to 1.4 μm. The critical grain size for a loss of ductility is

around 1 μm, which coincides with the previous result at a quasi-static strain rate of 8.3×10^{-4} s^{-1} [5]. In contrast, the total elongation has a tendency to increase with increasing the strain rate in all grain sizes. On the other hand, the change in the uniform elongation was somewhat complicated. When the grain size was larger than 1 μm, the uniform elongation increased with increasing the strain rate as well as the total elongation. When the grain size was submicrometer, the uniform elongation did not change. This indicates that the increase in the total elongation at high strain rates was mainly due to the increase in the uniform elongation for the specimens having the grain size coarser than 1 μm, while it was attributed to the increase in the post-uniform elongation for the submicrometer grain-sized specimens. The increase in uniform elongation can be explained in terms of the enhanced strain-hardening at higher strain rates that was described in the previous section.

Summary

Commercial purity aluminum sheets having various grain sizes from 0.20 to 10 μm were fabricated by the ARB and subsequent annealing process, and their tensile tests were carried out at strain rates ranging from 10^{-2} to 10^{3} s^{-1} (from ordinary quasi-static deformation to dynamic deformation). The major results obtained are summarized below:

(1) The UFG Al with mean grain size of 1.4 m exhibited the yield-drop phenomenon, which was unusual in the coarse-grained Al. The yield-drop phenomenon appeared more clearly at the higher strain rate. Besides this exceptional phenomenon, the yield stress was independent of the strain rate.

(2) The tensile strength had a tendency to increase with increasing the strain rate in all grain-sized specimens. The increase is significant at strain rates above 10^{2} s^{-1}. It was attributed to an enhancement of strain-hardening. The enhancement of strain-hardening was confirmed by the increase in dislocation density in the tensile-deformed specimens.

(3) The total elongation decreased with decreasing the grain size. The critical grain size for a large change in ductility was about 1 μm. The total elongation has a tendency to increase with increasing the strain rate in all grain sizes. The ductility increase was responsible for the uniform elongation in grain size above 1 μm, however, post-uniform elongation below 1 μm.

Acknowledgements The authors would like to thank for the financial supports by the Grant-in-Aid for Young Scientist (Start Up) (No. 18860051), Grant-in-Aid for scientific research from the ministry of education on priority areas "Giant straining process for advanced materials containing ultra-high density lattice defects", and Industrial Technology research Grain Program '05 through New Energy and Industrial Technology Development Organization (NEDO) of Japan (project ID: 05A27502d).

References

1. Altan BS, Miskioglu I, Purcek G, Mulyukov RR, Artan R (2006) Severe plastic deformation towards bulk production of nano-structured materials. NOVA Science Publishers, New York
2. Tsuji N, Saito Y, Lee SH, Minamino Y (2003) Adv Eng Mater 5:338. doi:10.1002/adem.200310077
3. Saito Y, Tsuji N, Utsunomiya Y, Sakai T, Hong HG (1998) Scr Mater 391:221
4. Saito Y, Utsunomiya H, Tsuji N, Sakai T (1999) Acta Mater 47:579. doi:10.1016/S1359-6454(98)00365-6
5. Tsuji N, Ito Y, Saito Y, Minamino Y (2002) Scr Mater 47:893. doi:10.1016/S1359-6462(02)00282-8
6. Lu L, Sui ML, Lu K (2000) Science 287:1463. doi:10.1126/science.287.5457.1463
7. Huang X, Hansen N, Tsuji N (2006) Science 312:249. doi:10.1126/science.1124268
8. Mayer MA, Mishra A, Benson DJ (2006) Prog Mater Sci 51:427. doi:10.1016/j.pmatsci.2005.08.003
9. Tsuji N (2007) J Nanosci Nanotechnol 7:3765. doi:10.1166/jnn.2007.025
10. Wang YM, Ma E (2004) Mater Sci Eng A 375–377:46. doi:10.1016/j.msea.2003.10.214
11. Wei Q, Cheng S, Ramesh KT, Ma E (2004) Mater Sci Eng A 381:71. doi:10.1016/j.msea.2004.03.064
12. Chen J, Lu L, Lu K (2006) Scr Mater 54:1913. doi:10.1016/j.scriptamat.2006.02.022
13. Vehoff H, Lemaire D, Schuler K, Waschkies T, Yang B (2007) Int J Mater Res 98:259
14. Tanimura S, Mimura K, Umeda T (2003) J Phys IV Fr 110:385. doi:10.1051/jp4:20020724
15. Kamikawa N (2006) PhD thesis. Osaka University
16. Hall EO (1970) Yield point phenomena in metals and alloys. Macmillan
17. Suzuki T (1968) In: Rosenfield AR, Hahn GT, Bement AL Jr, Jaffee RI (eds) Dislocation dynamics. McGraw-Hill Book Company, New York
18. Hansen N, Jensen DJ (1999) Philos Trans R Soc Lond A 357:1447. doi:10.1098/rsta.1999.0384
19. Humphreys FJ, Hatherly M (2002) Recrystallizaiton and related annealing phenomena, 2nd edn. Elsevier Science, UK